5-10-1996

48Ca Production in Matter Expanding from High Temperature and Density

B S. Meyer
Clemson University

Tracy D. Krishnan
Clemson University

Donald D. Clayton
Clemson University, claydonald@gmail.com

THE ASTROPHYSICAL JOURNAL, 462:825–838, 1996 May 10

^{48}Ca PRODUCTION IN MATTER EXPANDING FROM HIGH TEMPERATURE AND DENSITY

BRADLEY S. MEYER, TRACY D. KRISHNAN, AND DONALD D. CLAYTON
Department of Physics and Astronomy, Clemson University, Clemson, SC 29634-1911
Received 1995 July 18; accepted 1995 November 16

ABSTRACT

We calculate with a large nuclear reaction network the nuclear dynamics associated with the expansions and cooling of initially hot and dense matter. We study matter with neutron excess near that of ^{48}Ca, because one objective is to clarify the nucleosynthesis of that abundant neutron-rich nucleus, whose origin has been enigmatic. Expecting that supernovae provide the site of its origin, we take initial temperatures near $T_9 = 10$ but survey a wide range of initial densities, corresponding to a wide range in initial entropies. The highest entropies are probably associated with winds from newborn neutron stars in Type II collapse events, whereas the smallest entropies are probably associated with very high density Type Ia cores. Our survey objective is the analysis of the dynamics of the nuclear assembly as it cools, and how the correct description of it depends on the specific entropy.

We show that resultant abundances of neutron-rich nuclei are very poorly represented by nuclear statistical equilibrium (NSE). The deviations from NSE are governed by the number of heavy nuclei assembled during the expansion, which differs significantly from the number demanded by NSE at both high and low entropy. High-entropy expansions are shown to contain too few nuclei, with the result that ^{48}Ca cannot survive the expansion even though it would be expected to be abundant using NSE guidelines. Low-entropy expansions contain too many nuclei with respect to that guideline, with the result that ^{48}Ca is more abundant than expected. In this case it is especially significant that the ratio of ^{48}Ca to other major neutron-rich nuclei (e.g., ^{66}Zn, ^{82}Se) is substantially greater than NSE guidelines, which ameliorates overproduction limits from the latter. We show, furthermore, that the ^{48}Ca nucleus itself plays a key role in the nuclear dynamics. In the low-entropy expansion, which is the one to which we must look for ^{48}Ca origin, abundant ^{48}Ca is a refractory post, a local abundance maximum, with quasi-equilibria attached to it in both the upward-mass direction (setting their abundances) and in the downward-mass direction (setting the disintegration rate of ^{48}Ca, which governs the attempt to relax to NSE).

Although understanding the network is our key result, we discuss some immediate consequences of astrophysical importance. We argue that Type Ia cores must be the site of origin of ^{48}Ca, and track one dense explosion of an oxygen-neon core to show that it adjusts its neutron richness during the burning to values similar to those in our survey ($\eta = 0.17$) and that the network dynamics are identical to those identified in our survey. We also discuss significant implications for the correlated endemic isotopic anomalies in neutron-rich isotopes discovered in calcium-aluminum–rich inclusions from meteorites.

Subject headings: nuclear reactions, nucleosynthesis, abundances — supernovae: general

1. INTRODUCTION

The abundance and origin of ^{48}Ca is one of the long-standing puzzles of nucleosynthesis. The solution of that puzzle will provide a sensitive diagnostic into the circumstances of the synthesis event. This nuclide is very abundant: $N(^{48}\mathrm{Ca}) = 114$ on the scale $N(\mathrm{Si}) = 10^6$ (Anders & Grevesse 1989). It is 47.5 times more abundant than ^{46}Ca, the next-to-heaviest stable isotope; and it is even more abundant than ^{43}Ca, which is synthesized in the great main line of oxygen and silicon burning in supernovae (e.g., Weaver & Woosley 1993). It has 30% the abundance of prominent ^{42}Ca. It is not a rare nuclide.

^{48}Ca is also an extraordinarily neutron-rich species. It is the only stable nucleus below (and including) Fe that carries 8 excess neutrons. It is among the most neutron-rich nuclei known [$N-Z$ is $\frac{1}{6}$ of $N+Z$; i.e., $\eta(^{48}\mathrm{Ca}) = \frac{1}{6}$]. One must search up to ^{64}Ni before encountering another nuclide having 8 excess neutrons. The next naturally occurring isotope with $\eta \geq \frac{1}{6}$ is ^{82}Se. One then searches up to ^{96}Zr (two ^{48}Ca nuclei!) to find the next stable nucleus with η as large as $\frac{1}{6}$, and up to ^{116}Cd, an r-process species, to find the next naturally occurring species with $\eta > \frac{1}{6}$.

The extraordinary properties of ^{48}Ca are possible, of course, because calcium ($Z = 20$), a proton-magic element, is just able to reach neutron magic ($N = 28$) in the stability field. This doubly magic structure causes the binding energy per nucleon of ^{48}Ca to exceed that of ^{40}Ca and ^{42}Ca, and indeed of every isotope within all elements of lower atomic number! Five different elements (Ca, Ti, V, Cr, and Fe) have stable isotopes carrying 28 neutrons, a feat that does not recur until the magic $N = 50$ closed shell. Of the five $N = 28$ nuclei, ^{48}Ca is the lightest, with the heaviest (^{54}Fe) having a whopping 6 additional protons. The relatively large abundances of the $N = 50$ closed-shell nuclei can be attributed to the s-process of neutron capture; but this is not possible for ^{48}Ca, owing (among other things) to the 48-fold smaller abundance of ^{46}Ca, from which it must be generated on a slow-capture timescale. In their famous formulation of nucleosynthesis, Burbidge et al. (1957) attributed ^{48}Ca to the r-process, which creates neutron-magic abundance peaks away from the line of beta-decay stability. Sensing that idea not to be quite right, Cameron (1979) attributed it to neutron-rich silicon burning, a process that appears not to occur anywhere. Hartmann, Woosley, & El Eid (1985) therefore turned to the neutron-rich e-process

(nuclear statistical equilibrium [NSE]) in search of a source for ^{48}Ca. Although ^{48}Ca was shown to have mass fractions as large as $X(^{48}\mathrm{Ca}) = 0.1$ for neutron excesses near $\frac{1}{6}$ (to match ^{48}Ca), the overall situation is perilous. At neutron excesses as small as $\frac{1}{8}$, the ^{66}Zn overabundance would exceed that of ^{48}Ca by a factor of 6, and for neutron excesses as great as $\frac{1}{5}$, the ^{82}Se overabundance would exceed that of ^{48}Ca by a factor of 8. Other such problems exist in superpositions of matter in NSE having differing neutron richnesses.

The approach of this paper is to abandon reliance on nuclear statistical equilibrium and to examine the role of ^{48}Ca in expansions and cooling of very hot matter. We will show that it plays a significant role in the nuclear dynamics of neutron-rich expansions. What we will find is that for relatively fast expansions, such as have been found useful in understanding the origin of the *r*-process nuclei in hydrodynamic outflows (winds) from newly born neutron stars at the cores of Type II supernovae (Meyer et al. 1992; Takahashi, Witti, & Janka 1994; Woosley et al. 1994), the matter near ^{48}Ca is far from NSE. We will find that at relatively low entropy, abundant ^{48}Ca survives the expansion even when NSE suggests that it should not; and at high entropies, the ^{48}Ca is formed abundantly but cannot survive owing to deviations from NSE. Our attempts to understand this behavior have brought insights into ^{48}Ca synthesis that have come with difficulty, and that we herein explain.

To abandon NSE means that we will follow a nuclear reaction network from the initial moment of very hot matter to the final moments of reaction freezeout. Such expansions are most naturally characterized by the entropy per nucleon, s, because an adiabatic expansion conserves this quantity. The entropy, however, is often an unwieldy function of the temperature, matter density, and degree of neutron richness. We instead employ a related quantity, the number of photons per nucleon (ϕ, the photon-to-nucleon ratio). The ratio ϕ is a monotonically increasing function of the entropy per nucleon (e.g., Meyer 1993). To within factors of ~ 3, $\phi \sim 0.1s/k$, where k is Boltzmann's constant, for $\phi \gtrsim 0.1$, while $\phi \sim 0.01s/k$ for $\phi \lesssim 0.1$.

The quantity ϕ is conveniently written

$$\phi = 0.34 \frac{T_9^3}{\rho_5}, \qquad (1)$$

where T_9 is the temperature in 10^9 K and ρ_5 is the matter density in 10^5 g cm^{-3}. The relevance of ϕ can be easily grasped by considering some reference temperature, for example, $T_9 = 6$. The lower ϕ is, the greater the mass density when the matter passes through $T_9 = 6$. The larger ϕ is, the lower the reference density, and the higher will be the mass fractions in free alpha particles and nucleons. All this is well known (see, e.g., Meyer 1994); but we will show some fascinating features of the ^{48}Ca abundance and how it depends on the photon-to-nucleon ratio.

That the substantial abundance of ^{48}Ca probably comes from expansions of low-entropy matter leads us to speculate (along with others) that a rare class of Type Ia supernovae was responsible for its synthesis. We will show that constraints on ^{48}Ca synthesis based on coproduction of heavier isotopes such as ^{66}Zn are loosened by the breakdown of NSE that occurs at low entropy. In fact, ^{48}Ca synthesis at low entropy appears to be more robust than previously realized. These considerations have important implications for the ^{48}Ca anomalies found in calcium-aluminum–rich inclusions (CAIs) in meteorites.

2. CALCULATIONAL TECHNIQUES AND NUMERICAL RESULTS

The nucleosynthesis code used for the present studies is a fully implicit network code written by one of us (B. S. M.). The network used (see Table 1) included isotopes from the vicinity of the proton drip line to the neutron drip line for elements from hydrogen ($Z = 1$) to tin ($Z = 50$), a total of ~ 1350 species. Nuclear reaction rates are from Caughlan & Fowler (1988), Thielemann, Arnould, & Truran (1987), and Rauscher et al. (1994) where available. These rates are supplemented by approximations in Woosley et al. (1975) and Woosley & Hoffman (1992). Neutron-capture rates above krypton are from Bao & Käppeler (1987) and Cowan, Thielemann, & Truran (1991). Weak-interaction rates on intermediate-mass nuclei are from Fuller, Fowler, & Newman (1980, 1982a, 1985). Other experimental nuclear data, where available, are from Tuli (1990).

We also wrote a subroutine for the network code that computed NSE abundances at each time step of an expansion. The NSE subroutine used the same network, nuclear masses, and partition functions as the network code. With this routine we were able to compare the network abundances with those in NSE throughout an expansion. The abundances in the network code relax, given adequate time, to those computed from the NSE code under the appropriate conditions of high temperature and density.

We ran a series of calculations with ϕ ranging from 0.001 to 10. All calculations began at a temperature $T_9 = 10$ and a neutron excess $\eta = \frac{1}{6}$, the η of ^{48}Ca. We took ϕ to be constant during the expansion; thus, $\rho \propto T^3$ (see eq. [1]), where ρ is the mass density. Such a density-temperature relation is only strictly valid when relativistic particles dominate the

TABLE 1

NUCLEAR NETWORK EMPLOYED

Element	A_{min}	A_{max}	Element	A_{min}	A_{max}
n	1	1	Fe	47	75
H	1	3	Co	50	78
He	3	4	Ni	51	80
Li	6	9	Cu	57	85
Be	7	12	Zn	59	86
B	8	14	Ga	59	94
C	11	17	Ge	62	97
N	12	20	As	65	100
O	14	21	Se	68	103
F	18	22	Br	69	106
Ne	18	29	Kr	72	109
Na	19	32	Rb	74	113
Mg	20	37	Sr	76	118
Al	22	40	Y	78	121
Si	23	41	Zr	80	122
P	27	44	Nb	81	123
S	28	47	Mo	82	124
Cl	31	50	Tc	87	127
Ar	32	53	Ru	90	130
K	35	58	Rh	93	131
Ca	36	59	Pd	94	132
Sc	40	64	Ag	97	133
Ti	42	65	Cd	98	136
V	43	68	In	99	149
Cr	44	69	Sn	102	152
Mn	46	74			

entropy, that is, when $\phi \gtrsim 1$. Nevertheless, it is a convenient parametrization, and we use it throughout with the realization that fully hydrodynamic models of astrophysical settings for expansions of neutron-rich matter will no doubt have somewhat different temperature-density tracks. The time dependence of the density was taken to be $\rho \propto \exp(-t/\tau_{ex})$, where τ_{ex}, the expansion timescale, was 0.2 s in all calculations, except where noted. The density falloff timescale will differ from 0.2 s in more realistic astrophysical models, but 0.2 s is typically of the correct order of magnitude. In general, the results of low-entropy freezeout calculations are much more sensitive to ϕ and η than to τ_{ex}. In all cases we begin with alpha particles and enough neutrons to make $\eta = \frac{1}{6}$. The initial nuclear abundances are typically not important in these calculations, because the matter quickly attains NSE. Nevertheless, it takes some time for the matter to reach NSE, and this time is governed to some extent by ϕ and the initial abundances chosen.

Figure 1 shows $O(^{48}\mathrm{Ca})$, the final overproduction of ^{48}Ca in the expansions as a function of ϕ. (The overproduction factor of a species is the ratio of its mass fraction in the nucleosynthetic environment to that in the solar system.) For $\phi \lesssim 1$, ^{48}Ca is overproduced at a level $\sim 10^6$. These are extremely large overproductions. Indeed, for $0.002 \lesssim \phi \lesssim 1$, ^{48}Ca is the most overproduced isotope in these $\eta = \frac{1}{6}$ expansions. On the other hand, for $\phi \gtrsim 2$, the ^{48}Ca overproduction factors plummet. Furthermore, for $\phi > 1$, ^{48}Ca is no longer the most overproduced isotope. Rather, it is a heavier neutron-rich isotope such as ^{84}Kr, ^{86}Kr, or ^{90}Zr. For $\phi \lesssim 0.002$, enough electron captures occur to increase η significantly during the expansion, but for most of Figure 1 the final η is very near that of ^{48}Ca. The most overproduced isotope for $\phi = 0.001$ is ^{70}Zn, whose progenitor, ^{70}Ni, is more neutron-rich than ^{48}Ca.

Figure 1 also shows for comparison the NSE overproduction factors for ^{48}Ca assuming $\eta = \frac{1}{6}$ and an arbitrary freezeout temperature of $T_9 = 3.5$. Such NSE calculations have been used in the past to explore nucleosynthesis in neutron-rich ejecta (e.g., Hainebach et al. 1974; Hartmann et al. 1985). Obviously, the two curves differ. ^{48}Ca is overproduced relative to NSE for $\phi \lesssim 1$, while it is drastically underproduced relative to NSE for $\phi \gtrsim 1$. We seek to understand this. To do so, we analyze in detail two expansions, namely, $\phi = 5$ and $\phi = 0.3$. The former gives the $O(^{48}\mathrm{Ca})$ greatly below the NSE value, while the latter gives the maximum ^{48}Ca overproduction in the $\phi = 0.001$–10 range. By analyzing these two qualitatively different expansions, we will achieve a deeper understanding of the nucleosynthesis in expansions of hot, dense, neutron-rich matter.

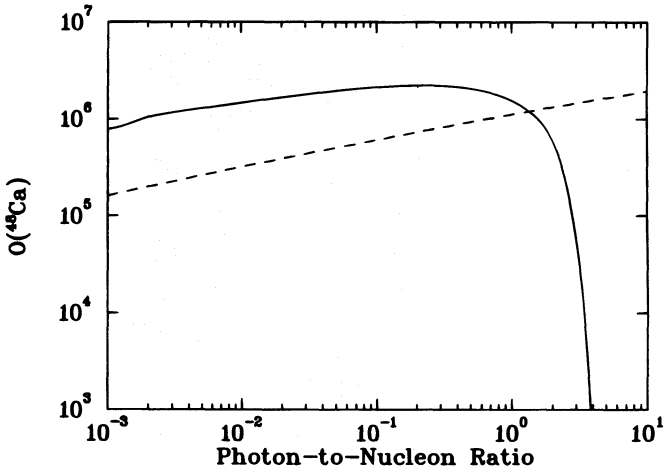

FIG. 1.—Overproduction $O(^{48}\mathrm{Ca})$ from the network expansion is compared with its overabundance in NSE (*dashed line*) as a function of the photon-to-baryon ratio ϕ (eq. [1]). For small ϕ ($\phi < 1$) the overproduction, near 10^6, is 3–5 times larger than NSE guidelines, whereas for large ϕ ($\phi > 2$) it is much less than NSE. Each expansion here uses initial $\eta = \frac{1}{6}$ to optimize ^{48}Ca production and 0.2 s density timescale.

2.1. $\phi = 5$ *Expansion*

We begin the analysis of the $\phi = 5$ expansion by first discussing two important reaction sequences, namely, $\alpha + \alpha + \alpha \rightarrow {}^{12}\mathrm{C}$ and $\alpha + \alpha + n \rightarrow {}^{9}\mathrm{Be}$ followed by $^{9}\mathrm{Be}(\alpha, n)^{12}\mathrm{C}$. Because of the lack of stable nuclear species at mass number 5 and 8, these reactions provide the gateways for synthesis of heavier nuclei for any system that starts (as in the present calculations) with neutrons and alpha particles. These three-body reactions are also the first important reactions to freeze out during an expansion, and this fact has profound consequences for the subsequent nuclear evolution.

Figure 2 shows the timescale for disappearance of an alpha particle due to the triple-alpha reaction and to the $\alpha + \alpha + n \rightarrow {}^{9}\mathrm{Be}$ reaction in the $\phi = 5$ expansion. For comparison, the short-dashed line shows the expansion timescale ($\tau_{ex} = 0.2$ s). The triple-alpha timescale becomes longer than τ_{ex} for $T_9 \approx 6.4$. Below this temperature, the triple-alpha reaction has frozen out. With this important gateway closed, the system can no longer assemble as many heavy nuclei as NSE demands; hence, NSE can no longer hold. Nevertheless, the sequence through ^{9}Be continues to operate and to assemble heavy nuclei down to $T_9 \approx 5.7$. Once the $\alpha + \alpha + n \rightarrow {}^{9}\mathrm{Be}$ reaction freezes out, however, so does the abundance Y_h of heavy nuclei (nuclei with mass number $A \geq 12$). This last consequence is a conceptual key.

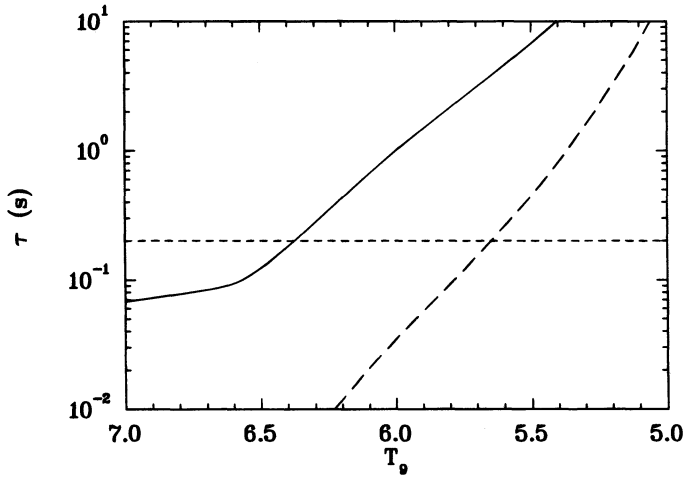

FIG. 2.—Alpha-consumption timescale τ, defined by $dY/dt = -Y/\tau$, set by triple-alpha reaction (*solid curve*) and by $\alpha + \alpha + n$ reaction (*long-dashed curve*) is displayed as a function of temperature for the $\phi = 5$ expansion. The alpha density (not shown) is of course also declining with T in accord with the $\phi = 5$ network, and contributes, along with T, to the declining consumption rate (increasing depletion timescale). The density e-folding time $\tau_{ex} = 0.2$ s is shown for comparison (*short-dashed curve*). The network becomes unable to consume alphas by triple-alpha as the temperature falls below $T_9 = 6.4$ and by $\alpha + \alpha + n$ below $T_9 = 5.7$. The alphas can be consumed only by such creation of new heavy nuclei, because their consumption by existing heavy nuclei is opposed almost exactly by the inverse reactions in established quasi-equilibria.

We may now explore these effects on the nuclear system. Figure 3*a* shows $X(^{48}\mathrm{Ca})$, the mass fraction of ^{48}Ca during the expansion. Also shown (*short-dashed curve*) is the NSE mass fraction of ^{48}Ca during the expansion. At $T_9 \approx 6.4$, the ^{48}Ca mass fraction deviates from that in NSE due to the freezeout of the triple-alpha reaction. $X(^{48}\mathrm{Ca})$ builds up to a level greater than 0.01 but falls dramatically below $T_9 \approx 6$ and levels off (freezes out) for $T_9 < 3$. The NSE mass fraction, on the other hand, remains fairly large until it falls drastically for $T_9 < 3$.

The destruction of ^{48}Ca *during the* $\phi = 5$ *expansion is not due to freezeout modifications of an underlying NSE distribution.* Rather, it is primarily the result of a shifting quasi-equilibrium (QSE; Bodansky, Clayton, & Fowler 1968; Woosley, Arnett, & Clayton 1973). In a QSE, there is a specific group of heavy nuclei that are in equilibrium with each other under exchange of alpha particles, neutrons, and protons; but they are not in equilibrium with those light particles themselves. The first evidence for this is from Figure 3*a*. The long-dashed curve shows the ^{48}Ca mass fraction during a $\phi = 5$ expansion if all proton-capture and alpha-capture rates on all Ca isotopes are decreased by a factor of 100. The final mass fraction of ^{48}Ca in this case is $\sim 10^2$ times greater, but the previous approximately 10^3-fold decline of ^{48}Ca from $T_9 \approx 6$ to $T_9 \approx 4$ proceeds exactly as before and is therefore clearly not due to the rates of proton-capture or alpha-capture reactions. In fact, throughout much of the expansion, the abundances are distributed in a QSE in which there is a nearly exact balance between forward and reverse reactions (except the three-body reactions). This is possible because the individual two-body reaction rates are rapid compared to the timescale on which the system changes dynamically. For example, at $T_9 = 5.24$, the $^{48}\mathrm{Ca}(\alpha, n)^{51}\mathrm{Ti}$ reaction timescale is 2.82×10^{-8} s. The timescale for the reverse reaction, $^{51}\mathrm{Ti}(n, \alpha)^{48}\mathrm{Ca}$, at this temperature is 8.91×10^{-9} s. These timescales are much shorter than τ_{ex}, and QSE is easily maintained. QSE exists down to $T_9 \approx 4.3$, at which point the two-body reactions freeze out and destroy the QSE. It is only this freezeout that was altered (Fig. 3*a*) by the rescaling of nuclear rates.

How does the QSE lead to destruction of ^{48}Ca? The consequence of early freezing out of the three-body reactions involving alpha particles is that the system cannot consume the alphas to make heavy nuclei as quickly as NSE demands. Figure 3*b* shows X_α, the mass fraction of alpha particles, during the expansion and the corresponding NSE alpha mass fraction. For $T_9 \lesssim 6.4$, we see that the system has the expected excess of alphas compared to NSE. The alphas freeze out at a mass fraction of $\sim 10^{-4}$, so this expansion is an alpha-rich freezeout (Woosley et al. 1973).

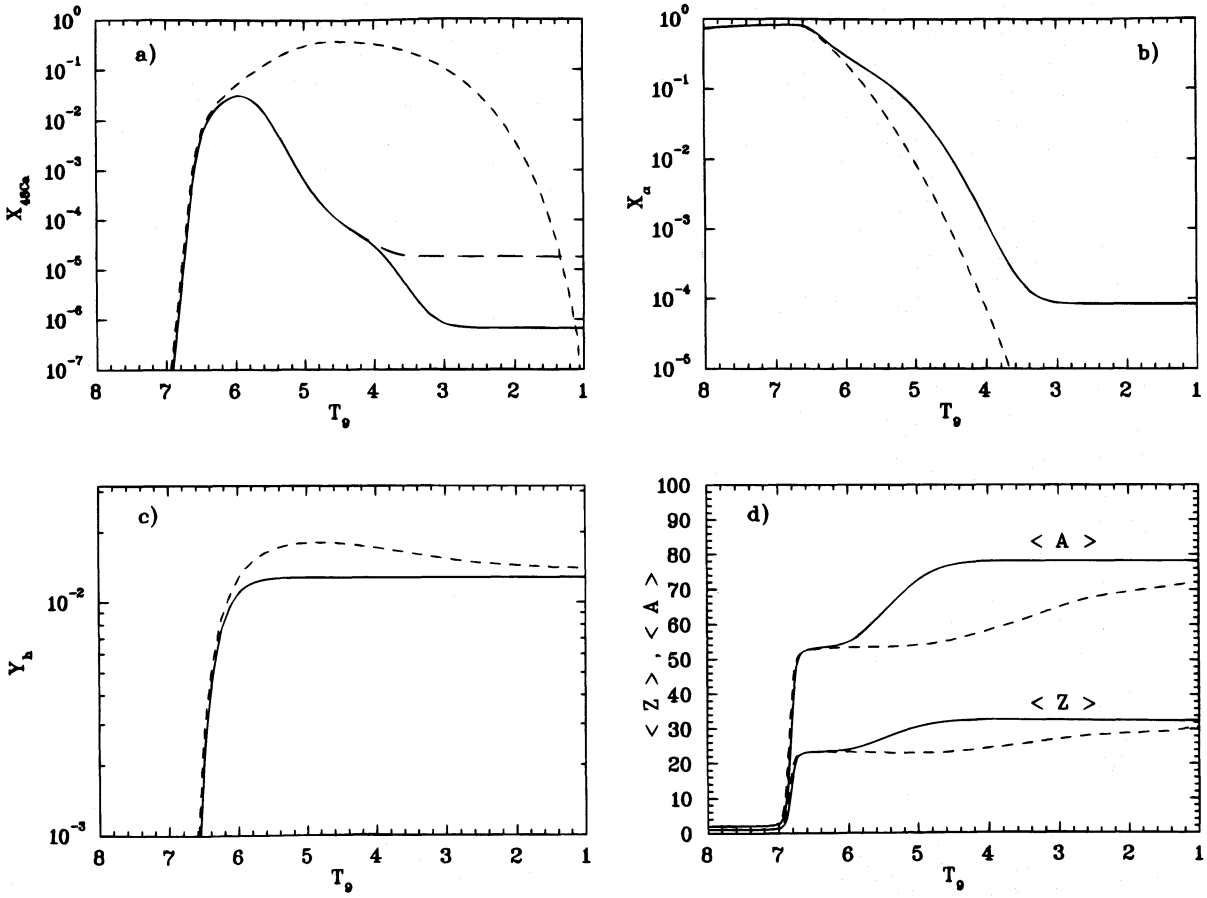

FIG. 3.—Evolution of abundances as a function of declining temperature for the $\phi = 5$ expansion. (*a*) The mass fraction of ^{48}Ca (*solid curve*) follows NSE guidelines above $T_9 = 6.4$, but plummets below NSE (*short-dashed curve*) below $T_9 = 6$, when alpha consumption becomes slow (Fig. 2). The long-dashed curve shows that decreasing all proton and alpha reaction rates with Ca by a factor of 100 makes no difference until very late, with final freezeout reactions below $T_9 = 4$. By that time the ^{48}Ca had already disappeared by a shifted quasi-equilibrium. (*b*) The alpha mass fraction (*solid curve*) is increasingly greater than the NSE guideline (*dashed curve*) as temperature falls, owing to the growing inability to consume them. (*c*) Abundance per baryon of (all) heavy nuclei, Y_h, settles into a nearly constant value that is less than NSE (*dashed curve*). (*d*) Mean atomic weight and mean charge of the heavy nuclei becomes larger than their NSE guidelines as the temperature falls below $T_9 = 6$, owing to the deficiency in their abundance at $\phi = 5$.

The new conceptual aspect not recognized in prior calculations (e.g., Woosley & Hoffman 1992) of neutron-rich, alpha-rich freezeouts is the quasi-equilibrium abundance distribution attached to ^{48}Ca, and that its evolution, rather than freezeout reactions, governs the resulting nucleosynthetic yields.

The excess of alpha particles compared to NSE translates into an underabundance of heavy nuclei, as seen in Figure 3*c*. The network and NSE abundances Y_h of heavy nuclei diverge at $T_9 \approx 6.4$ due to the quenching of the triple-alpha reaction, while Y_h in the expansion freezes out at $T_9 \approx 5.7$ due to the quenching of $\alpha + \alpha + n \rightarrow {}^9\mathrm{Be}$. At $T_9 \approx 5$, Y_h in the expansion is $\sim 50\%$ less than in NSE. There exist only two-thirds of the heavy nuclei demanded by NSE.

Because of the excess of alphas and the deficit of heavy nuclei, QSE favors heavier nuclei than does NSE. As a specific example, at the same temperature and density, the ratio $(^{64}\mathrm{Ni}/^{48}\mathrm{Ca})_{\mathrm{QSE}}$ is larger than the corresponding ratio $(^{64}\mathrm{Ni}/^{48}\mathrm{Ca})_{\mathrm{NSE}}$ by the ratio $(Y_\alpha^{\mathrm{QSE}}/Y_\alpha^{\mathrm{NSE}})^4$, which gets large quickly (Fig. 3*b*) as T_9 falls below 6. This promotes a shift of QSE abundance from ^{48}Ca to ^{64}Ni. This is demonstrated in a more general way in Figure 3*d*. At $T_9 \approx 5$, NSE favors nuclei with an average proton number $\langle Z \rangle \approx 21$ and mass number $\langle A \rangle \approx 54$, while the nuclei in the network calculation actually have $\langle Z \rangle \approx 30$ and $\langle A \rangle \approx 80$. We see clearly that the destruction of ^{48}Ca is primarily not a freezeout effect but rather a shifting QSE. One must envision it as a broad abundance peak shifting to another, heavier, broad abundance peak containing the same number of nuclei.

The NSE Y_h drops after $T_9 \approx 5$. NSE's goal as the temperature falls is to assemble nuclei with the largest binding energy per nucleon consistent with the degree of neutron richness of the system (e.g., Meyer 1994). For $\eta = \frac{1}{6}$, this is a combination of ^{66}Ni ($\eta = 0.1515$) and ^{82}Se ($\eta = 0.1707$). Thus, as T_9 drops, NSE also favors nuclei heavier than ^{48}Ca (see Fig. 3*d*). Because the number of nucleons is a constant, their NSE rearrangement into heavier nuclei necessarily requires a decrease in the number of nuclei. In actual expansions, however, the number of heavy nuclei cannot change in the time available.

Figure 4 further elucidates the nuclear evolution of this high-entropy expansion. Shown are Y_Z, the abundance of nuclei with proton number Z, versus Z for various temperatures during the expansion. Early in the expansion, at $T_9 = 6.09$, the distribution fairly closely matches that of NSE. By $T_9 = 5.78$, there is a noteworthy deficiency of lighter nuclei ($20 \leq Z \leq 25$) and an excess of heavier nuclei ($30 \leq Z \leq 35$) relative to NSE. By $T_9 = 5.12$. the difference between the QSE and NSE distributions is dramatic. Because the system has not been able to assemble as many nuclei as NSE demands, the overabundance of light particles forces the nuclei to larger Z. By $T_9 = 2.01$, the expan-

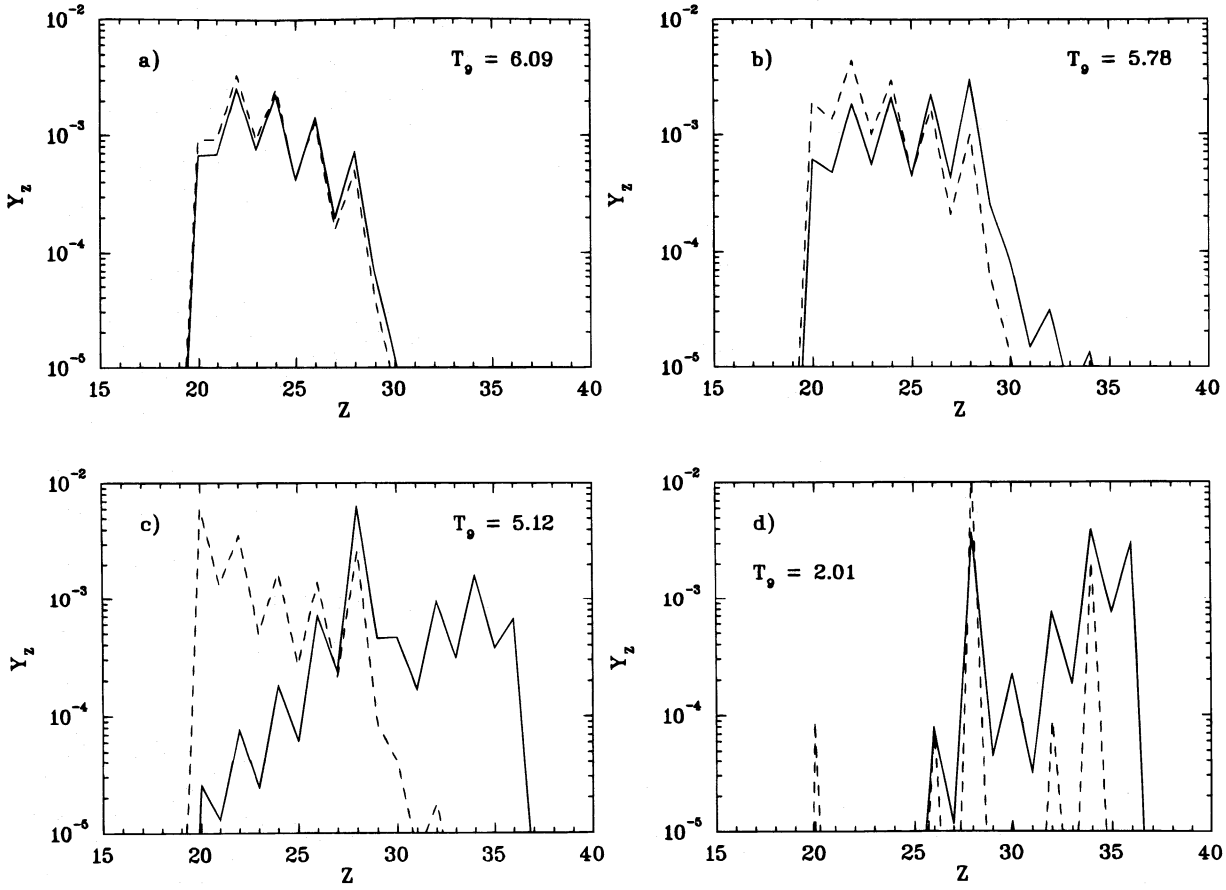

FIG. 4.—Abundance per baryon of each element Z, displayed in panels of falling temperature in the high-entropy $\phi = 5$ case: (*a*) $T_9 = 6.09$, (*b*), $T_9 = 5.78$, (*c*) $T_9 = 5.12$, and (*d*) $T_9 = 2.01$. The NSE expectation is also shown (dashed curve) at each T. Instead of NSE, the heavy nuclei are in QSE with each other under exchanges of alpha particles, neutrons, protons and gammas, but are not in equilibrium with the abundances of those light particles. The quasi-equilibrium at $T_9 = 5.12$ (*c*) is shifted from a Ca-dominated one for NSE to a heavy-element–dominated one. The final distribution is seen much enriched above $Z = 28$ (Ni) with respect to NSE. These are primarily quasi-equilibrium patterns with excess alphas, rather than the results of freezeout reactions with excess alphas.

sion abundances have frozen out and the shifting NSE distribution has moved to higher mass, as discussed previously.

If QSE does indeed hold, then we may tie the abundance of any heavy nucleus ^AZ to that of ^{48}Ca by

$$Y(^AZ) = Y(^{48}\mathrm{Ca})C(Z, A, T_9, \phi)(X_n)^{A-Z-28}(X_p)^{Z-20} \quad (2)$$

(Bodansky et al. 1968; Woosley et al. 1973), where $C(Z, A, T_9, \phi)$ is a function of its arguments and X_p and X_n are the mass fractions of free protons and neutrons, respectively. Similarly, in NSE

$$Y^{\mathrm{NSE}}(^AZ) = Y^{\mathrm{NSE}}(^{48}\mathrm{Ca})C(Z, A, T_9, \phi) \times (X_n^{\mathrm{NSE}})^{A-Z-28}(X_p^{\mathrm{NSE}})^{Z-20}, \quad (3)$$

where C is the same function in equations (2) and (3). A convenient diagnostic for determining the degree of quasi-equilibrium with ^{48}Ca is then

$$R(Z, A) \equiv \left[\frac{Y(^AZ)/Y(^{48}\mathrm{Ca})}{Y^{\mathrm{NSE}}(^AZ)/Y^{\mathrm{NSE}}(^{48}\mathrm{Ca})}\right] \times \left(\frac{X_p}{X_p^{\mathrm{NSE}}}\right)^{20-Z}\left(\frac{X_n}{X_n^{\mathrm{NSE}}}\right)^{28+Z-A}. \quad (4)$$

If a nucleus (Z, A) is in precise quasi-equilibrium with ^{48}Ca, then $R(Z, A) = 1$. Figure 5 shows that at $T_9 = 5.12$ nearly all nuclei with $Z > 15$ are in tight QSE with ^{48}Ca and thus that the destruction of ^{48}Ca is due to the shifting QSE.

If we consider ^{66}Ni, then it must be true in QSE that $R_{66} = 1$, where $R_{66} = R(28, 66)$ is given by

$$R_{66} \equiv \left[\frac{Y(^{66}\mathrm{Ni})/Y(^{48}\mathrm{Ca})}{Y^{\mathrm{NSE}}(^{66}\mathrm{Ni})/Y^{\mathrm{NSE}}(^{48}\mathrm{Ca})}\right]\left(\frac{X_p}{X_p^{\mathrm{NSE}}}\right)^{-8}\left(\frac{X_n}{X_n^{\mathrm{NSE}}}\right)^{-10}. \quad (5)$$

Figure 6 shows X_n, X_n^{NSE}, X_p, and X_n^{NSE}, while Figure 7 shows R_{66} during the expansion. That R_{66} is so close to unity down to $T_9 \approx 4.3$ shows the tight QSE that holds among the heavy nuclei down to freezeout. The light-particle ratios could, if one chooses, also be written $(X_\alpha/X_\alpha^{\mathrm{NSE}})^{-4}(X_n/X_n^{\mathrm{NSE}})^{-2}$, with precisely the same conclusion.

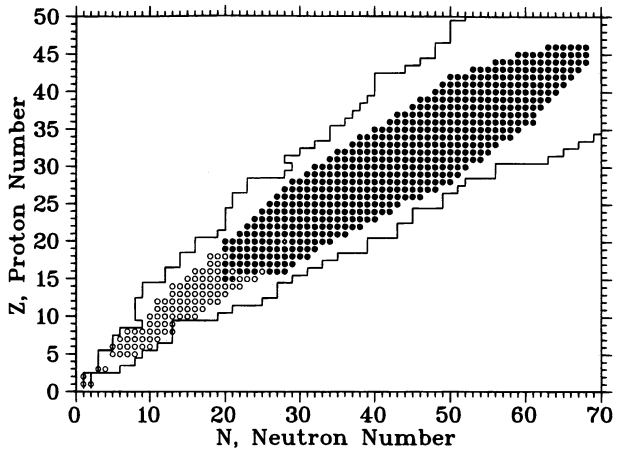

FIG. 5.—Extent of the QSE for the $\phi = 5$ expansion at $T_9 = 5.12$ in the neutron number–proton number plane. The solid lines give the range of the nuclear reaction network (see Table 1). Nuclides (excluding n, p, α) with a mass fraction greater that 10^{-20} at this point in the expansion are marked by an open or filled circle. A filled circle indicates that $R(Z, A)$ (see eq. [4]) for that nuclide lies within a factor of 2 of unity [$0.5 \lesssim R(Z, A) \lesssim 2$]. These nuclei are then in a tight quasi-equilibrium with ^{48}Ca (*open diamond*). Open circles indicate nuclides not in tight quasi-equilibrium with ^{48}Ca. Clearly, a tight QSE exists between P ($Z = 15$) and Pd ($Z = 46$). Because this QSE exists at a point in the expansion where ^{48}Ca is being destroyed (see Fig. 3*a*), the destruction of ^{48}Ca is due to a shifting QSE rather than to freezeout reactions with excess alphas.

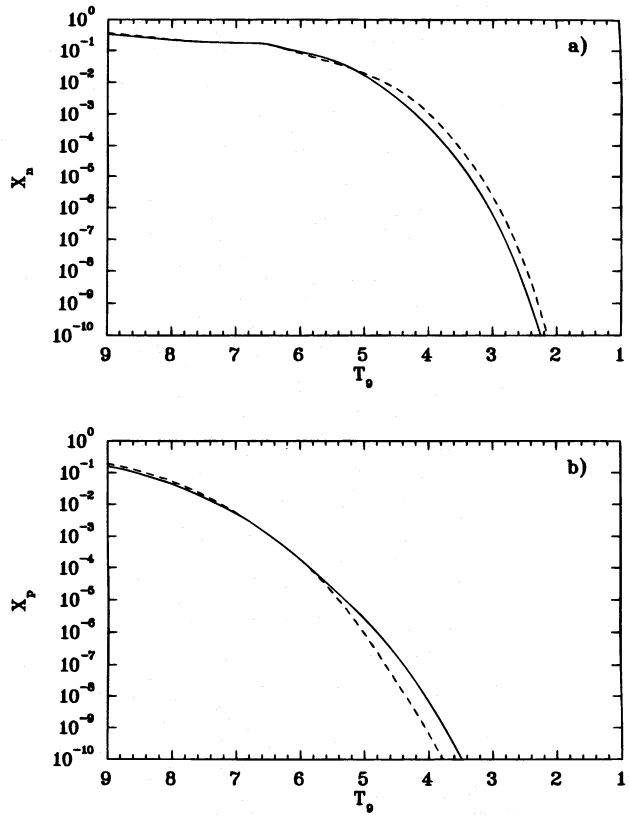

FIG. 6.—Neutron and proton mass fractions during $\phi = 5$ evolution (*solid curve*) are compared to their NSE counterparts (*dashed curve*). Neutrons are slightly less abundant than in NSE because they are more tightly bound in the heavy nuclei above Z = 28 than in the lighter NSE distribution (see Fig. 4). The protons are more abundant than in NSE because they are more tightly bound in lighter nuclei with smaller Coulomb energy. These deviations are exactly consistent with the alpha excess (Fig. 3*b*) and equilibrium between particles, neutrons, and protons (see eq. [6]).

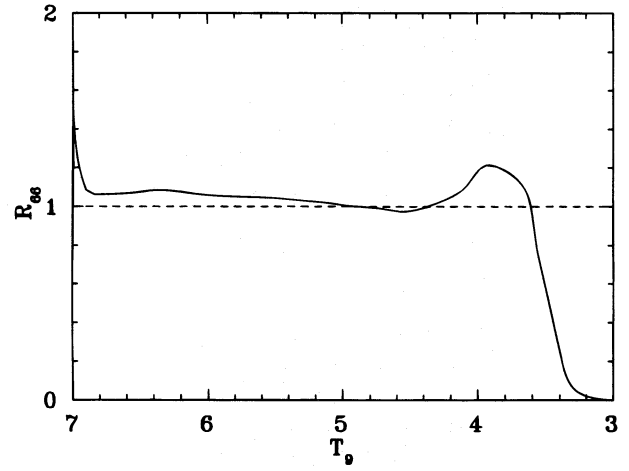

FIG. 7.—Ratio R_{66} measuring the goodness of the quasi-equilibrium between ^{48}Ca and ^{66}Ni (see eq. [5]). Its value is unity when QSE holds, and is exactly unity in NSE (*dashed line*). Quasi-equilibrium remains tight down to almost 4×10^9 K, when final freezeout reactions consume a small portion of the remaining alphas (Fig. 3*b*).

Further inspection of Figure 6 reveals that $X_n < X_n^{NSE}$ for $T_9 < 5$. On the other hand, $X_p > X_p^{NSE}$. This must be so in order that $X_\alpha > X_\alpha^{NSE}$. Indeed, in QSE the neutrons and protons are in equilibrium with the alpha particles so that $X_\alpha \propto X_n^2 X_p^2$. If we define

$$R \equiv \left(\frac{X_\alpha}{X_\alpha^{NSE}}\right)\left(\frac{X_n}{X_n^{NSE}}\right)^{-2}\left(\frac{X_p}{X_p^{NSE}}\right)^{-2}, \quad (6)$$

QSE demands $R = 1$. Figure 8 shows R versus T_9 for the $\phi = 5$ expansion. For $4.3 \lesssim T_9 \lesssim 6.4$, R is extremely close to unity. This shows the tight equilibrium among neutrons, protons, and alpha particles. Surprisingly, $R > 1$ for $T_9 > 6.9$. This is due to the fact that the system is not in NSE for $T_9 > 6.9$. It began with too many alpha particles. Although normally one would expect that the system should be in NSE at these high temperatures and densities, we began the calculations at $T_9 = 10$ out of NSE (with alphas and neutrons rather than primarily neutrons and protons). This system actually required some 0.2 s to reach NSE, by which point the temperature had dropped to $T_9 = 7$. That NSE is not a given for high temperatures and densities is a useful caveat.

In Figure 8 we have summarized the phases of the $\phi = 5$ expansion. From $T_9 = 10$ down to $T_9 \approx 6.9$, the system works its way into NSE from its initial composition. NSE then holds down to $T_9 \approx 6.4$, at which point the triple-alpha reaction freezes out. The other reactions continue to occur quickly, however, so that QSE holds. At $T_9 \approx 5.7$, the $\alpha + \alpha + n \rightarrow {}^9$Be reaction and, consequently, the abundance Y_h of heavy nuclei both freeze out. In the QSE phase, which lasts down to $T_9 \approx 4.3$, the nuclei are overweight with respect to those in NSE. Finally, below $T_9 \approx 4.3$, the individual two-body reactions freeze out and QSE can no longer hold. By this time, however, ^{48}Ca had already disappeared because the QSE had been endowed with too few nuclei!

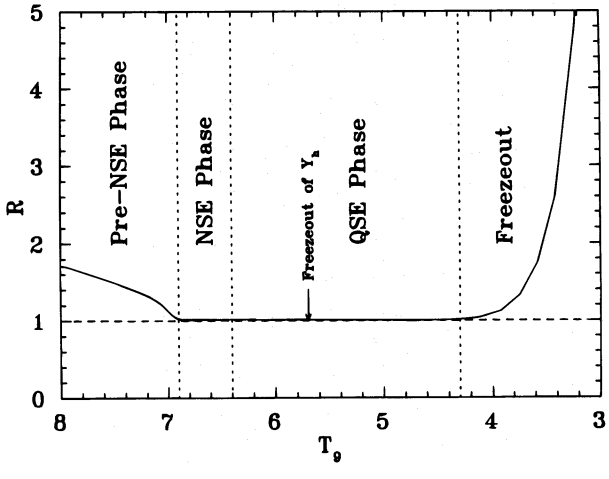

FIG. 8.—Nuclear epochs of the $\phi = 5$ expansion. The ratio R measures the goodness of the equilibrium between alpha particles, neutrons, and protons during the high-entropy expansion. Its value is unity when the equilibrium holds. It remains tight down to 4×10^9 K. The deviations from unity occur above 7×10^9 K as a result of the initial conditions without protons; but NSE has been established by $T_9 = 7$. This tight equilibrium is maintained during NSE (down to $T_9 = 6.4$), during the quasi-equilibrium epoch (down to 4.3×10^9 K). At the end, R again becomes large as excess alphas remain unconsumed. Another marked moment of interest is the freezeout of the total number of heavy nuclei, which occurs during the QSE phase near 5.7×10^9 K.

Table 2 summarizes the result of the $\phi = 5$ expansion at $\eta = \frac{1}{6}$ by listing the overabundances of the most overproduced isotopes. Beta-decays have already occurred, so that only stable daughters are listed. The table contains all overproductions within 0.1% of the maximum overproduction (^{86}Kr). These isotopes are, as Woosley & Hoffman (1992) noted, quite heavy in comparison with NSE.

In order to explore the sensitivity of our results to τ_{ex}, we ran two other $\phi = 5$ expansions at $\eta = \frac{1}{6}$, but with different expansion timescales. The first was with a 10 times faster expansion ($\tau_{ex} = 0.02$ s). The overproduction factors for this calculation are also shown in Table 2. The nuclei produced are larger in mass than in the $\tau_{ex} = 0.2$ s expansion. This is because the faster expansion leads to an earlier quenching of the triple-alpha and $\alpha + \alpha + n$ reactions and, consequently, a quicker freezeout of the number of nuclei. The higher temperature freezeout for $\tau_{ex} = 0.02$ s leads to even fewer nuclei and more light particles compared to NSE, and the QSE nuclear distribution thus shifts to even larger nuclear mass than in the $\tau_{ex} = 0.2$ s expansion.

The second variation on the $\phi = 5$, $\eta = \frac{1}{6}$ expansion was with a 10 times slower expansion ($\tau_{ex} = 2.0$ s). The overproduction factors for this expansion are also shown in

TABLE 2

OVERPRODUCTION FACTORS FOR $\phi = 5.0$ EXPANSIONS

	τ_{ex}		
^AZ	0.2 s	0.02 s	2.0 s
^{48}Ca	...	...	5.78×10^5
^{49}Ti	...	...	7.04×10^3
^{64}Ni	...	...	8.39×10^4
^{63}Cu	...	...	6.55×10^3
^{66}Zn	3.90×10^5	...	1.12×10^5
^{67}Zn	1.76×10^4	...	8.13×10^4
^{68}Zn	2.30×10^4	...	8.97×10^5
^{70}Zn	1.07×10^5	...	2.22×10^6
^{69}Ga	5.61×10^4	...	9.12×10^5
^{71}Ga	...	...	1.01×10^6
^{72}Ge	2.31×10^5	...	8.58×10^4
^{73}Ge	...	...	2.95×10^5
^{74}Ge	...	...	3.45×10^5
^{76}Ge	2.42×10^5	...	2.12×10^5
^{75}As	1.46×10^5	...	5.07×10^4
^{77}Se	7.07×10^4	...	1.39×10^6
^{78}Se	1.78×10^6	...	4.85×10^5
^{80}Se	4.31×10^4	...	1.67×10^6
^{82}Se	8.69×10^6	...	1.10×10^5
^{79}Br	4.35×10^4	...	8.61×10^4
^{81}Br	1.19×10^6	...	9.05×10^5
^{83}Kr	1.21×10^5	1.05×10^5	1.52×10^6
^{84}Kr	4.10×10^6	1.56×10^6	1.96×10^6
^{86}Kr	1.55×10^7	3.18×10^5	1.67×10^4
^{85}Rb	5.66×10^6	1.15×10^6	2.52×10^5
^{87}Rb	5.93×10^4	7.99×10^6	...
^{88}Sr	...	4.72×10^6	...
^{89}Y	...	6.22×10^6	...
^{90}Zr	...	3.25×10^7	...
^{91}Zr	...	1.60×10^6	...
^{94}Zr	...	9.63×10^5	...
^{96}Zr	...	4.81×10^6	...
^{93}Nb	...	9.07×10^5	...
^{95}Mo	...	1.11×10^5	...
^{97}Mo	...	1.70×10^5	...
^{98}Mo	...	1.86×10^5	...
^{100}Mo	...	1.14×10^5	...
^{99}Ru	...	9.21×10^5	...
^{102}Ru	...	8.99×10^4	...
^{103}Rh	...	3.27×10^4	...

Table 2. In this expansion the abundances are shifted to lower nuclear mass than those in the $\tau_{ex} = 0.2$ s expansion. This results from the later, or lower temperature, freezeout of the number of nuclei. Because of the later freezeout, more nuclei are produced in the expansion than in the $\tau_{ex} = 0.2$ s expansion. In the subsequent QSE phase, the nuclei are in equilibrium under exchange of a smaller number of light particles than in the $\tau_{ex} = 0.2$ s expansion, so the QSE abundance distribution does not shift to as large a nuclear mass.

In summary, the overproductions from high-entropy expansions are quite sensitive to the expansion timescale. On the other hand, for none of the calculations with $\phi = 5$ and $\eta = \frac{1}{6}$ did ^{48}Ca dominate the overproductions. We may safely conclude that ^{48}Ca does not come from high-entropy, neutron-rich expansions.

2.2. $\phi = 0.3$ *Expansion*

The $\phi = 0.3$ expansion differs from the $\phi = 5$ expansion in an extremely interesting way. In matter that expanded and cooled from high temperature to low temperature and always managed to maintain NSE, the final abundances are dominated by the nuclei with the greatest binding energy per nucleon consistent with the degree of neutron richness of the system (typically a combination of ^{66}Ni, ^{68}Ni, and ^{82}Se for $\eta = \frac{1}{6}$). We thus might not expect much ^{48}Ca to remain in expansions with $\eta = \frac{1}{6}$ (e.g., Hartmann et al. 1985). Nevertheless, Figure 1 shows that in network expansions the ^{48}Ca is richly overproduced. In fact, it is the most overproduced isotope for $0.002 \lesssim \phi \lesssim 1$. This remarkable result warrants further thought. It can be traced to an important difference between low-entropy and high-entropy expansions, namely, that high-entropy expansions tend to freeze out with too few nuclei while low-entropy expansions freeze out with too *many* nuclei! We believe that this last fact has not been previously appreciated and that it bears significant astrophysical consequences.

As with the $\phi = 5$ expansion, we first note the timescales for the crucial three-body reactions in the $\phi = 0.3$ expansion. These are shown in Figure 9. The triple-alpha reaction freezes out for $T_9 \approx 6.5$, while the $\alpha + \alpha + n \rightarrow {}^9$Be reaction sequence freezes out for $T_9 \approx 6.2$. One might be surprised

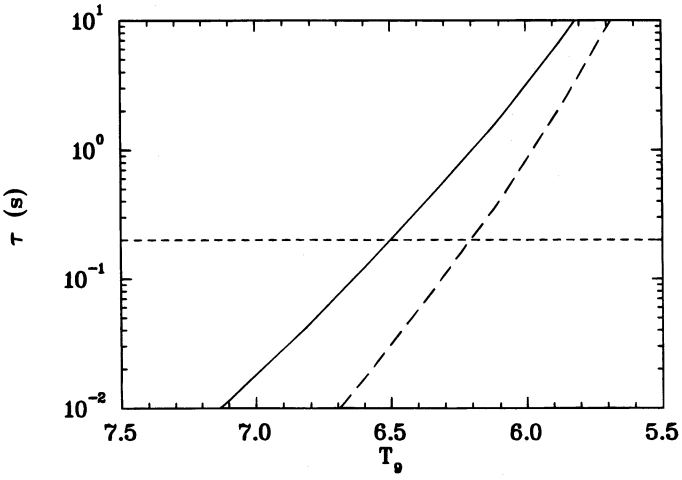

FIG. 9.—Timescale for alpha depletion for a higher density expansion ($\phi = 0.3$). The triple-alpha reaction (*solid curve*) becomes slower than the expansion below $T_9 = 6.5$, and the ^{9}Be branch does so below 6.2×10^9 K. Below that the production of additional nuclei stops.

that the triple-alpha reaction freezes out at roughly the same T_9 as in the $\phi = 5$ expansion. The density is about 17 times higher in the $\phi = 0.3$ case, which suggests a faster reaction and a lower freezeout temperature. On the other hand, the abundance of alpha particles is about 17 times smaller for $\phi = 0.3$ at $T_9 \approx 6.5$, which counters the larger density.

Figure 10 compares key abundances with NSE for the $\phi = 0.3$ expansion. From Figure 10*a*, we see that $X(^{48}\text{Ca}) \approx 0.3$ at the end of the expansion. This is in contrast to the mass fraction of ^{48}Ca in NSE of $\sim 10^{-7}$ at $T_9 = 1$. The ^{48}Ca mass fraction in the expansion diverges from NSE at $T_9 \approx 6.5$, due to the triple-alpha reaction freezeout, and even more strikingly at $T_9 = 5$, when the expansion comes to have too many nuclei.

That the $\phi = 0.3$ expansion freezes out with too many nuclei is apparent in Figures 10*c* and 10*d*. Figure 10*c* shows that there are fewer heavy nuclei in the system from $T_9 \approx 6.5$ to $T_9 \approx 4.8$ than in NSE. This occurs for the same reason as in the $\phi = 5$ expansion: the three-body reactions involving alpha particles start to freeze out and keep the system from assembling as many heavy nuclei as NSE demands. The system is still in QSE at these temperatures, however. Below $T_9 \approx 4.8$, the abundance of heavy nuclei in NSE drops below the network heavy nuclei abundance, which is unchanging. The charge and mass of the average nucleus in NSE are increasing (Fig. 10*d*) as the system cools, causing it to evolve toward abundances dominated by ^{66}Ni, ^{68}Ni, and ^{82}Se. In order to do this, the nucleons must rearrange themselves. Because the number of nucleons is constant, an increase in the average mass of the nuclei means that their number must decrease. On the other hand, in the network expansion, the network is unable to make this rearrangement in the available time.

Figure 11 further clarifies the picture. At $T_9 = 5.87$, the distribution of nuclei in the network expansion is shifted to slightly larger Z than in NSE. This is due to the fact that the system is in QSE with a deficit of heavy nuclei and an excess of alpha particles at this point. At $T_9 \approx 4.78$, the abundance of heavy nuclei happens to be almost exactly the same in the network expansion and in NSE. At this temperature, the distribution of nuclei in the network expansion matches the NSE distribution. Below $T_9 = 4.78$, the NSE distribution shifts to larger Z than the network distribution. By $T_9 = 2.06$, the network abundances have frozen out. They greatly differ from the NSE distribution. Of tremendous importance is the fact that the abundance of calcium is extremely large.

Why is the expanding system unable to keep up with NSE in this case? The answer bears some resemblance to the solution to silicon burning. In silicon burning, NSE favors ^{56}Ni, but the system has ^{28}Si. Clearly, the system has more nuclei than NSE demands, and it is thermodynamically favorable for the nucleons in ^{28}Si to rearrange themselves into ^{56}Ni. The obvious reaction channel $^{28}\text{Si} + {}^{28}\text{Si} \rightarrow {}^{56}\text{Ni}$, in principle open in NSE, is much too slow in any real environment due to the huge Coulomb barrier for this reaction. What must happen is that some of the ^{28}Si nuclei disintegrate into alpha particles. These alpha particles are then captured onto the remaining ^{28}Si nuclei to produce the ^{56}Ni.

An analogous situation is present in our $\phi = 0.3$ expansion. Below $T_9 \approx 4.78$, the ratio of free alpha particles to heavy nuclei is $\lesssim 0.01$; therefore, the nuclei do not have enough free alpha particles to capture to increase their

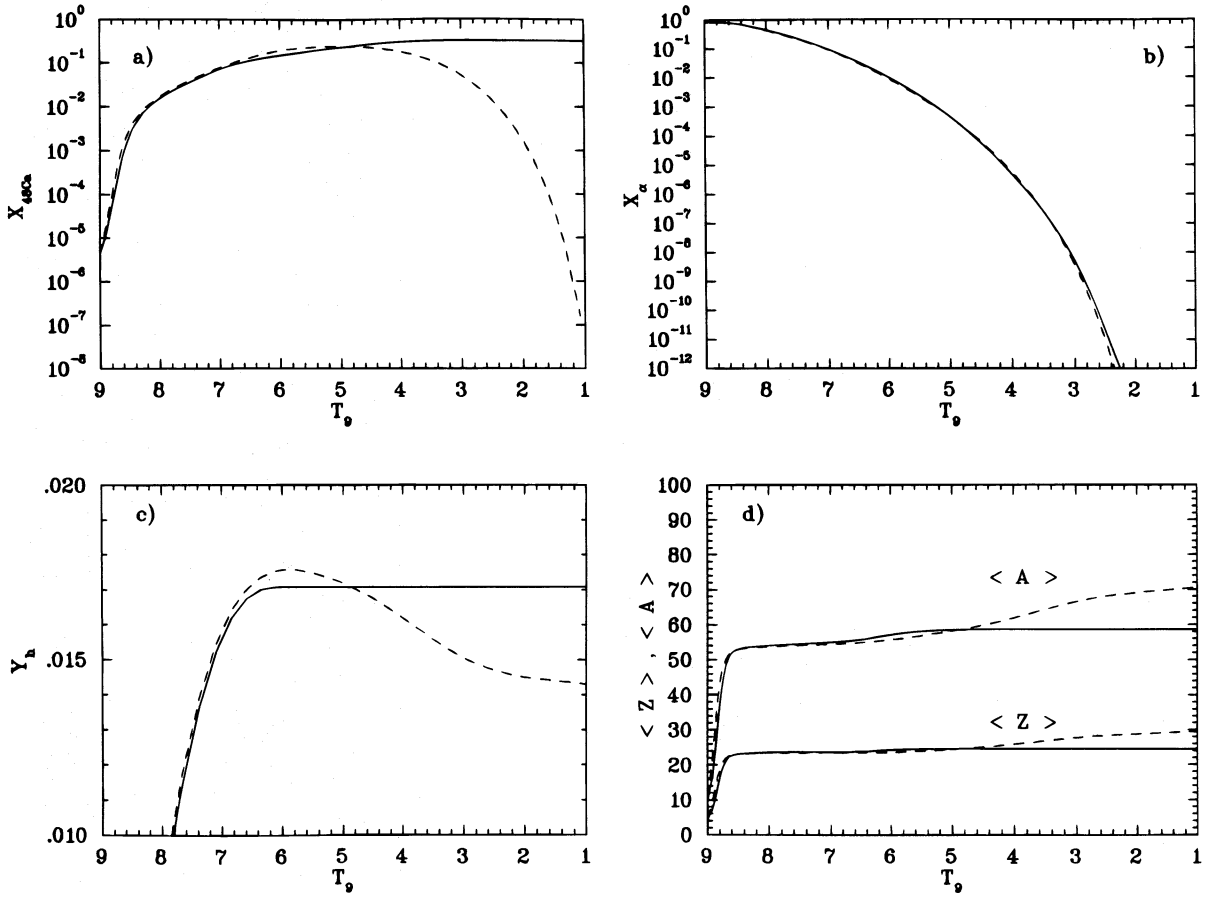

FIG. 10.—Evolution of abundances as a function of declining temperature for the low-entropy example, $\phi = 0.3$. (*a*) Although the ^{48}Ca mass fraction is near (on this log scale) the NSE value (*dashed curve*) above 4.6×10^9 K, it remains an astonishingly large $X(^{48}\text{Ca}) = 0.3$ at the end, whereas its value would have plummeted in NSE. (*b*) The alpha mass fraction is near NSE. (*c*) The total number of heavy nuclei is too large for NSE guidelines below 5×10^9 K, and their number cannot be reduced in the time remaining. (*d*) The mean atomic weight and charge (*solid curves*) become less than their NSE counterparts (*dashed curve*) below 5×10^9 K because their number is too great.

charges as NSE demands. Some of the nuclei must be disintegrated to provide light particles for the other nuclei to capture.

These disintegrations do occur. This is apparent in comparison of Figures 11*b*–11*d*. The abundances, Y_Z, of all elements with $20 \leq Z \leq 40$ dropped from $T_9 = 4.78$ to $T_9 = 2.06$, except for calcium ($Z = 20$; grew by 22%), nickel ($Z = 28$; grew by 21%), and selenium ($Z = 34$; grew by 30%). The growth of the abundance of nickel and selenium isotopes was in accord with the dictates of NSE, but the levels of growth were not those NSE required. Moreover, not only was the system unable to convert calcium (primarily ^{48}Ca) entirely into nickel (primarily ^{66}Ni) and selenium (primarily ^{82}Se), as NSE demanded, but the calcium abundance grew!

While the thermodynamic impetus of the material at $T_9 < 4.78$ is to disintegrate ^{48}Ca to make ^{66}Ni, ^{68}Ni, and ^{84}Se, the timescale to do so is very long. This is not because individual nuclear reactions are too slow. The ^{48}Ca(n, α)^{45}Ar reaction timescale is 2×10^{-6} s at $T_9 = 4.78$, which is considerably more rapid than $\tau_{ex} = 0.2$ s. The reason for the slowness is the fact that the matter is still in QSE, and forward rates are almost exactly balanced by reverse rates. The extent of the QSE is shown in Figure 12. Because the QSE includes the region between Ca and Mg, the effective disintegration rate of ^{48}Ca is governed by disintegration rates of smaller abundances in the Mg region, although we did not identify the relative importance of differing, specific, nuclear bottlenecks. This situation again bears similarity to Si burning, where the effective photodisintegration of ^{28}Si is governed by that of ^{24}Mg, and even of lighter nuclei for T_9 as great as 5 (Bodansky et al. 1968). The net disintegration timescale of ^{48}Ca is therefore $\gg \tau_{ex}$. For this reason, the system is unable to decrease the number of nuclei.

As the temperature falls in the expansion, the timescale to achieve NSE becomes even longer, and NSE becomes an even more hopelessly unreachable goal. Eventually, individual nuclear reactions become too slow and QSE freezes out. The system has never been able to decrease the number of nuclei as NSE required, and thus ^{48}Ca was able to survive. Not only has ^{48}Ca survived, it is seen as a key nucleus, the post on which the Y_h QSE is attached, and whose photodisintegration is slowed by the tiny-abundance QSE for $Z < 20$. Its role in "incomplete NSE" is analogous in these respects to that of ^{28}Si in "incomplete Si burning."

The reason ^{48}Ca actually increases in abundance after $T_9 = 4.78$ is that ^{48}Ca is, in its local region ($18 \lesssim Z \lesssim 24$), the most strongly bound nucleus for $\eta = \frac{1}{6}$. As the temperature drops, it therefore becomes even more favored in QSE. Net photodisintegration flows into it from above are arrested. It becomes a local abundance maximum, with declining QSEs dropping off in both directions in A. This is completely counter to the demands of NSE, but, again, NSE, unlike QSE in the present expansion, is assumed able

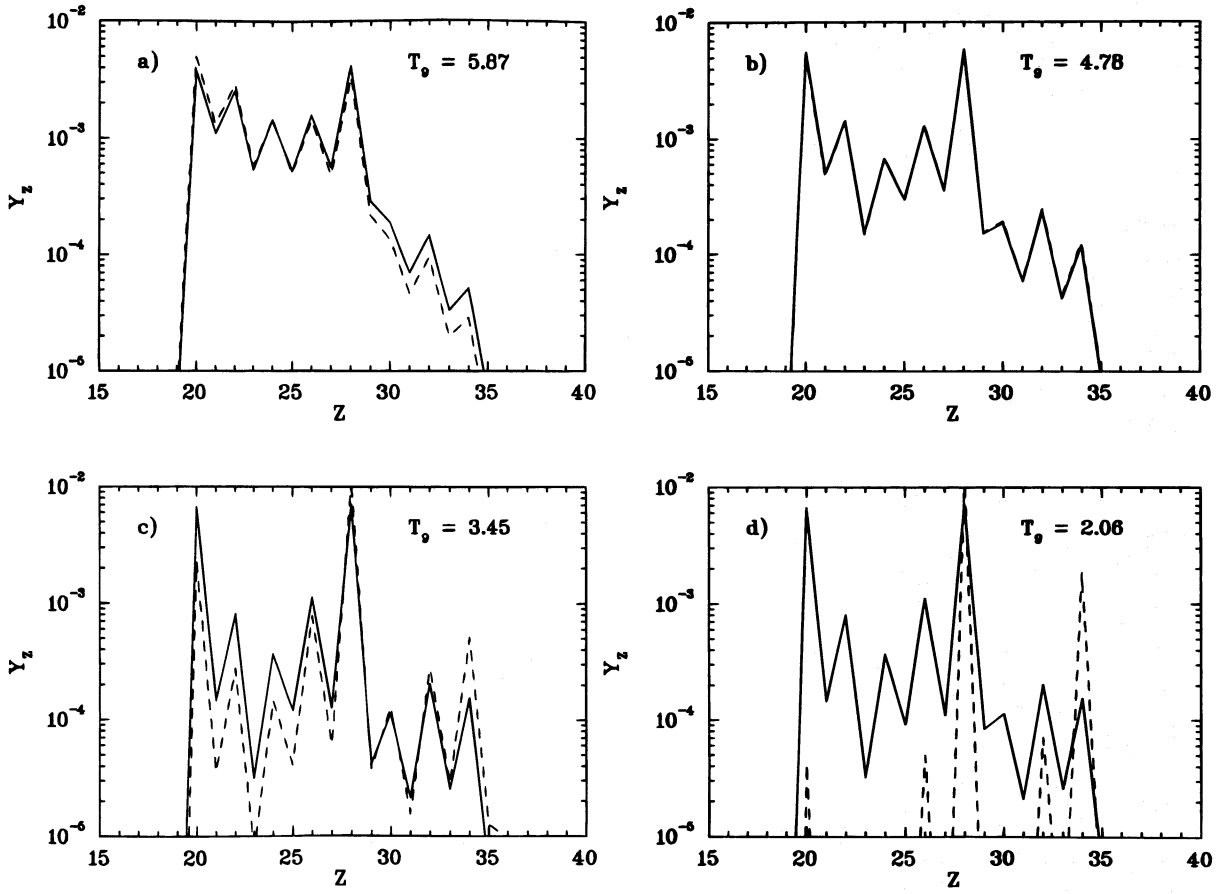

FIG. 11.—Elemental abundance distribution for $\phi = 0.3$. Temperatures are (*a*) $T_9 = 5.87$, when the nuclei are a little heavier than NSE (*dashed curve*), because at this early time they are still underabundant with respect to NSE; (*b*) $T_9 = 4.78$, when the distribution is almost exactly NSE, but just passing through (see Fig. 10*c*); (*c*) $T_9 = 3.45$, when the distribution has more intermediate-mass nuclei (Ca) and fewer heavy nuclei than NSE; and (*d*) $T_9 = 2.06$, frozen into a much broader distribution than NSE, with much more Ca and less ^{66}Ni and ^{82}Se. This shows why the ratio of ^{48}Ca to ^{66}Zn or ^{82}Se is much greater than NSE guidelines would lead one to expect in low-entropy expansions (e.g., Type Ia cores).

to adjust the number of nuclei. The abundance of ^{48}Ca also grows a little during freezeout ($\sim$3%). This is due again to the strong binding of ^{48}Ca, which makes the capture and disintegration reactions that produce this nuclide typically faster than those that destroy it.

Figures 13 and 14 show R_{66} and R for $\phi = 0.3$. The freezeout from QSE at $T_9 \approx 4$ is readily apparent. Also evident is the "pre-NSE phase" for $T_9 \gtrsim 9$. Again, this is because of our (non-NSE) initial conditions. The system reaches NSE before the triple-alpha reaction freezes out at $T_9 \approx 6.5$, so all traces of the initial abundances have disappeared before the QSE phase commences. It is, therefore, approximately valid for such low-entropy expansions to begin with NSE with $T_9 \gtrsim 6.5$ and to follow the subsequent QSE with a reaction network; but it is not valid to regard this as what have been called "freezeout corrections of NSE," and it would be very wrong to begin with the NSE near $T_9 = 4$. These systems have a more far-reaching memory than has been commonly supposed.

Table 3 summarizes the largest overproductions for the medium-entropy $\phi = 0.3$ expansion. The most overabundant final product is ^{48}Ca. The table lists stable daughters only, and only within 0.1% of the maximum overabundance. Also shown in Table 3 are the overproductions from a 10 times faster expansion ($\tau_{ex} = 0.02$ s) and a 10 times slower expansion ($\tau_{ex} = 2.0$ s). We find that over a 2 order of magnitude variation in expansion timescale, the variation in the overproduction factors is small and ^{48}Ca is always the most overproduced nucleus. Our conclusion that ^{48}Ca is made in low-entropy or medium-entropy expansions is not sensitive to the expansion timescale.

3. DISCUSSION

Our results have important implications for the site of synthesis of ^{48}Ca and for observation of isotopic anomalies in calcium-aluminium–rich inclusions (CAIs) in meteorites.

3.1. *Site of* ^{48}Ca *Synthesis*

The neutron-rich environment near the mass cut in a Type II supernova has long been a leading possible site for synthesis of ^{48}Ca (Hartmann et al. 1985). This environment is now known to have a high entropy ($s/k > 10$ or $\phi > 1$), however. Its high entropy results from heating by neutrinos from the cooling nascent neutron star (Bethe & Wilson 1985). We have shown that ^{48}Ca does not survive in such an environment: the material freezes out with too few nuclei, and the QSE that establishes itself favors nuclei heavier than ^{48}Ca. We can therefore rule out this Type II site as an origin for ^{48}Ca, even in matter having the neutron richness of ^{48}Ca.

What we seek instead for the synthesis site of ^{48}Ca is a *low-entropy*, neutron-rich environment. In such an environment, expanding material freezes out with too many nuclei

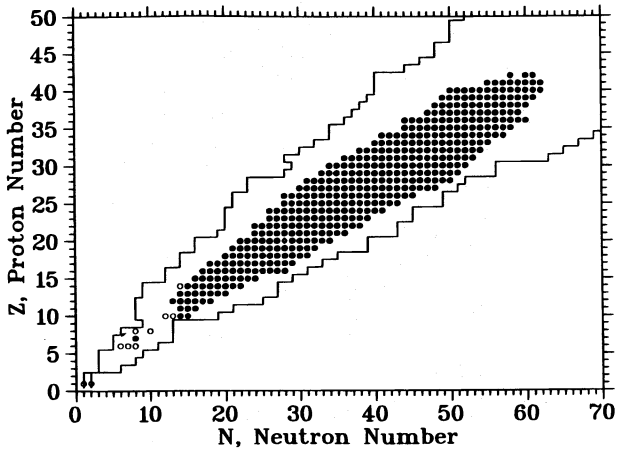

FIG. 12.—Extent of the QSE for the $\phi = 0.3$ expansion at $T_9 = 3.91$ in the neutron number–proton number plane. The solid lines give the range of the nuclear reaction network (see Table 1). Nuclides (excluding n, p, α) with a mass fraction greater than 10^{-20} at this point in the expansion are marked by an open or filled circle. A filled circle indicates that $R(Z, A)$ (see eq. [4]) for that nuclide lies within a factor of 2 of unity [$0.5 \lesssim R(Z, A) \lesssim 2$]. These nuclei are then in a tight quasi-equilibrium with ^{48}Ca (*open diamond*). Open circles indicate nuclides not in tight quasi-equilibrium with ^{48}Ca. Clearly, a tight QSE exists between Ne ($Z = 10$) and Mo ($Z = 42$). This QSE exists at a point in the expansion where the thermodynamic impetus is to disintegrate ^{48}Ca to provide light particles to allow the abundance distribution to shift to higher Z (see Figs. 11*b* and 11*c*). Because of the QSE below Ca, however, disintegration reactions are nearly exactly balanced by their reverse (capture) reactions, and the net disintegration rate of ^{48}Ca is extremely small. This explains why ^{48}Ca survives low-entropy expansions.

relative to NSE, which allows copious production of ^{48}Ca. Woosley & Eastman (1995) have called attention to such a site, namely, the cores of a certain rare class of Type Ia supernovae (deflagrations or detonations of C/O or O/Ne/Mg white dwarf stars). If the central density of the white dwarf star is high enough at ignition ($\rho \gtrsim$ a few times 10^9 g cm^{-3}), electron captures on heavy nuclei will make the matter neutron rich. Because of the high density, the material naturally has a low photon-to-nucleon ratio ($\phi \approx 0.001$–0.003).

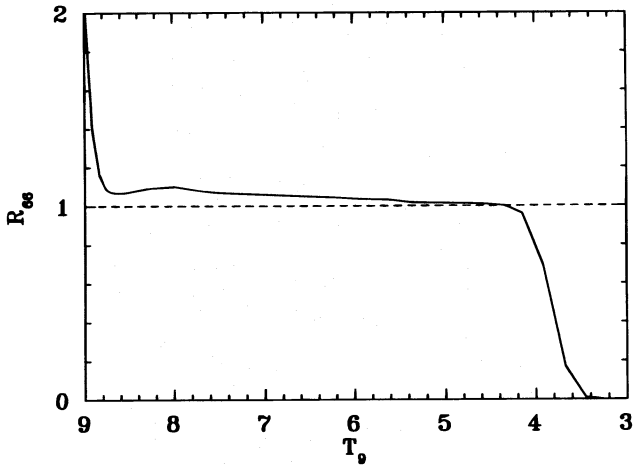

FIG. 13.—Ratio R_{66} measuring the goodness of the quasi-equilibrium between ^{48}Ca and ^{66}Ni (see eq. [5]). Its value is unity when QSE holds and is exactly unity in NSE (*dashed line*). QSE is a good approximation down to 4×10^9 K, when the ratio ^{66}Ni/^{48}Ca is unable to remain as large as its NSE value.

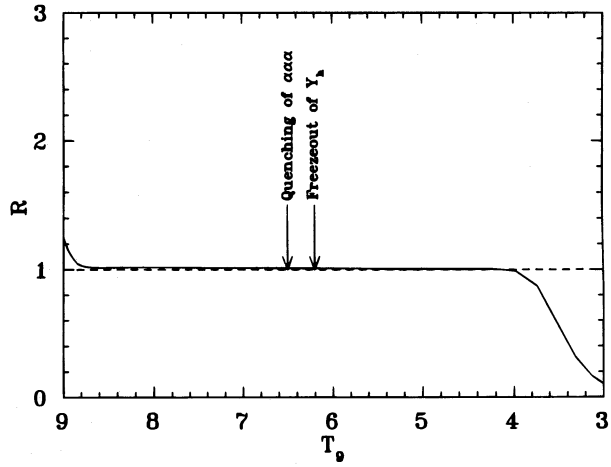

FIG. 14.—Ratio R measuring the goodness of the equilibrium between alphas, neutrons, and protons. This equilibrium is tight down to 4×10^9 K. A pre-NSE phase lasts from $T_9 = 10$ down to $T_9 \approx 8.8$, during which the initial non-NSE composition works its way into NSE. The NSE phase in this expansion lasts from $T_9 \approx 8.8$ down to triple-α quenching ($T_9 = 6.5$). Then comes the QSE phase, lasting until freezeout ($T_9 \approx 4$). The number of heavy nuclei freezes out at $T_9 \approx 6.2$.

We tested the Type Ia hypothesis with a low-entropy expansion. The calculation began with an initial temperature $T_9 = 8$ and $\phi = 1.74 \times 10^{-3}$, that is, a density $\rho = 10^{10}$ g cm^{-3}. This is a much lower entropy than in the preceding survey. We took the expansion timescale to be $\tau_{ex} = 1$ s and the initial composition to be 50% by mass of both ^{16}O and ^{20}Ne. The initial composition was actually

TABLE 3

OVERPRODUCTION FACTORS FOR $\phi = 0.3$ EXPANSIONS

	τ_{ex}		
^AZ	0.2 s	0.02 s	2.0 s
^{48}Ca	2.32×10^6	1.99×10^6	2.20×10^6
^{49}Ti.....	4.20×10^4	4.91×10^4	4.78×10^4
^{50}Ti.....	1.50×10^4	1.74×10^4	3.67×10^4
^{51}V	2.84×10^3	3.92×10^3	3.67×10^3
^{52}Cr	2.58×10^3	2.74×10^3	2.58×10^3
^{61}Ni	6.12×10^3	1.09×10^4	...
^{62}Ni	3.39×10^3	3.95×10^3	2.30×10^3
^{64}Ni	7.10×10^4	7.92×10^4	2.92×10^4
^{63}Cu	3.15×10^3	3.09×10^3	1.10×10^4
^{65}Cu	2.59×10^3	4.46×10^3	...
^{66}Zn	4.09×10^5	3.93×10^5	6.59×10^5
^{67}Zn	9.78×10^4	1.51×10^5	8.40×10^4
^{68}Zn	5.63×10^5	6.02×10^5	2.95×10^5
^{70}Zn	3.10×10^5	4.63×10^5	4.66×10^4
^{69}Ga	1.11×10^5	8.50×10^4	3.81×10^5
^{71}Ga	3.62×10^4	3.78×10^4	3.64×10^4
^{72}Ge	5.75×10^4	7.47×10^4	5.60×10^4
^{73}Ge	3.30×10^3	4.96×10^3	...
^{74}Ge	5.85×10^4	7.99×10^4	2.00×10^4
^{76}Ge	9.32×10^3	1.69×10^4	3.26×10^3
^{75}As	1.66×10^4	2.79×10^4	1.34×10^4
^{77}Se	1.53×10^5	2.52×10^5	4.23×10^4
^{78}Se	2.48×10^5	3.09×10^5	2.08×10^5
^{80}Se	1.39×10^5	1.88×10^5	3.93×10^4
^{82}Se	1.96×10^4	2.74×10^4	3.27×10^4
^{79}Br	1.32×10^4	2.22×10^4	6.82×10^3
^{81}Br	1.31×10^5	1.85×10^5	8.41×10^4
^{83}Kr	5.09×10^4	8.00×10^4	1.15×10^4
^{84}Kr	2.33×10^5	2.72×10^5	1.54×10^5
^{86}Kr	1.60×10^4	2.29×10^4	1.75×10^4
^{85}Rb	4.33×10^4	6.25×10^4	4.03×10^4

irrelevant because the matter achieved NSE within $\sim 10^{-10}$ s, and its neutron richness is produced during the burning. The initial density is greater than that found in the special Type Ia models expected to produce ^{48}Ca (Woosley & Eastman 1995), but the temperature-density tracks in these models run more like $\rho \propto T^{3/2}$, which causes the matter to stay at higher density for a given temperature than in our model. Our higher initial density compensates for this effect somewhat. During the expansion, the neutron richness η grew with time due to electron captures on heavy nuclei, as shown in Figure 15.

The resulting overproduction factors of the five most overproduced isotopes are shown in Table 4. ^{48}Ca, ^{50}Ti, and ^{66}Zn are all coproduced to within 25%. The large production of the two lighter isotopes is due to the matter freezing out with too many nuclei, as shown in § 2.2. In this particular run, the network froze out with $Y_h = 0.0169$, but the corresponding Y_h in NSE at $T_9 = 3.5$ is 0.0159, dropping further to 0.0154 at low temperature. The constraint of excess nuclei makes the ratio of ^{48}Ca and ^{50}Ti to heavy neutron-rich nuclei much greater than would be expected on the basis of NSE. This helpfully curtails the otherwise limiting overproduction of ^{66}Zn and ^{84}Kr.

The excellent coproduction of ^{48}Ca and related neutron-rich isotopes in this model leads us to agree with Woosley & Eastman (1995) that a class of Type Ia supernovae is a promising site of synthesis of ^{48}Ca. Indeed, they are even more promising than realized, because the ^{48}Ca overproduction is even more robust at low entropy and is spread over a wider range of η than NSE dictates. Because the overproductions of ^{48}Ca are so large, only some small fraction of Type Ia supernovae can be responsible for ^{48}Ca synthesis. These are presumably the few white dwarf stars that have high enough density at the time of ignition for electron captures to make neutron-rich matter.

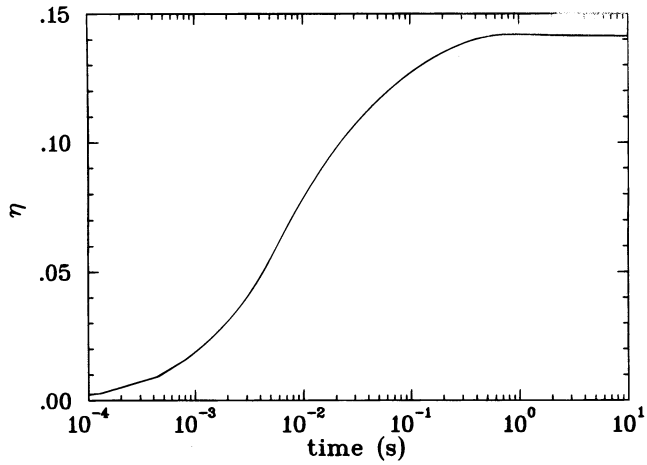

FIG. 15.—Evolution of the neutron excess during the simulation with the network of an O/Ne white dwarf. The neutron richness grows during the burning by electron captures, reaching values very close to those used in our survey.

TABLE 4

TOP FIVE OVERPRODUCTION FACTORS FOR TYPE Ia MODEL

^AZ	$O(^AZ)$
^{66}Zn	7.16×10^5
^{50}Ti	6.98×10^5
^{48}Ca	5.93×10^5
^{54}Cr	1.71×10^5
^{64}Ni	8.69×10^4

3.2. *CAIs*

That ^{48}Ca comes from expansion of low-entropy material has profound implications for observations of isotopic anomalies in CAIs (Lee, Papanastassiou, & Wasserburg 1978). Refractory mineralized inclusions within carbonaceous meteorites commonly have isotopic anomalies at ^{48}Ca, ^{50}Ti, and ^{54}Cr (e.g., Lee 1988). These are roughly correlated, in the sense that excess ^{48}Ca associates with excess ^{50}Ti and excess ^{54}Cr, positive and negative, but not in a strictly proportional way. This rough correlation has indicated that these isotopes are associated during nucleosynthesis, as theory maintains. Lack of direct proportionality and other factors related to molecular clouds and the solar accretion disk make interpretation by direct injection of anomalous matter from one nucleosynthesis event difficult. Clayton (1981) presented a chemical-memory alternative that may be endemic in interstellar dust from the historic spectrum of nucleosynthesis events.

We focus on the most immediately relevant issue of the present work for CAIs, namely, the loosening of NSE constraints on ^{48}Ca synthesis due to previously expected overproduction of heavier isotopes, especially ^{66}Zn. As we have seen, in low-entropy expansions with $\eta = \frac{1}{6}$, NSE favors nuclei such as ^{66}Ni, the progenitor of ^{66}Zn, ^{68}Ni, and ^{82}Se. Loss & Lugmair (1990) showed that the large expected correlations of excess ^{66}Zn with the other neutron-rich isotopes do not routinely exist; but Volkening & Papanastassiou (1990) found one inclusion having excess ^{66}Zn, and it was, in that one inclusion, correlated with but smaller than that at ^{48}Ca. Roughly speaking, these papers concluded that either the ^{66}Zn/^{48}Ca nucleosynthesis expectations were unrealistically large, or chemical memory is the correct model but Zn memory is weaker than Ca memory, or both. Our results have confirmed the former, but we also expect the latter. In the low-entropy expansions calculated by us, the freezeouts having too many nuclei cause production of lighter isotopes, such as ^{48}Ca, to be much greater relative to heavier isotopes like ^{66}Zn than inferred from NSE. We now understand that the anticipated overproduction of ^{66}Zn with respect to the other isotopes is an artifact of NSE calculations not necessarily applicable to real expansions.

Figure 16 shows this point more clearly. It gives the ratio of the overproduction of ^{66}Zn to that of ^{48}Ca in our series of $\eta = \frac{1}{6}$ expansions. For $\phi \lesssim 2$, ^{66}Zn is *underproduced* relative to ^{48}Ca in the network expansions. This is in contrast with the NSE results, which show ^{66}Zn *overproduced* relative to ^{48}Ca for $\phi \lesssim 0.1$.

We have studied how our conclusions depend on the degree of neutron richness. We ran constant $\phi = 0.03$ expansions from $T_9 = 10$ to freezeout for a large range of values of η. Since η is a time-varying quantity in these expansions, we characterized the results by the neutron richness as the material passed through $T_9 = 3.5$, approximately the temperature at which freezeout of strong and electromagnetic reactions occurred. Figure 17*a* shows the overproduction factors of only those stable daughter species that achieve the maximum overproduction (relative to all other species) somewhere in the range $\eta = 0.1$–0.3. Many species such as ^{66}Zn, which is, owing to its special interest,

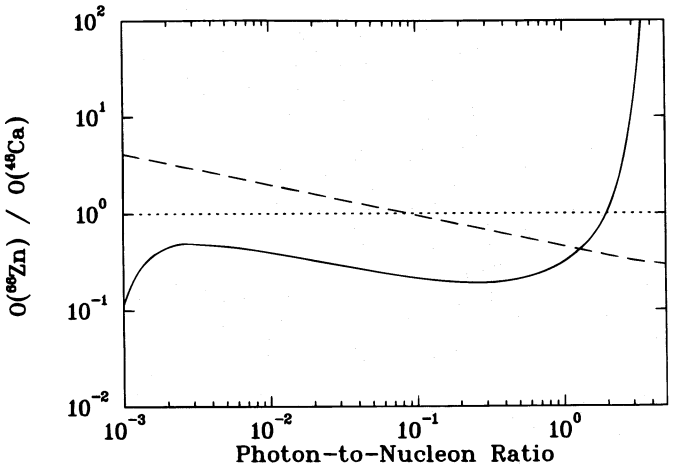

FIG. 16.—Ratio of final overproductions of ^{66}Zn to ^{48}Ca for low-entropy expansions (measured by photon-to-nucleon ratio ϕ; eq. [1]). For a wide range of ϕ-values characteristic of white dwarf ignitions, $O(^{66}\mathrm{Zn})/O(^{48}\mathrm{Ca})$ is a factor of 3–5 less than NSE guidelines (*long-dashed line*). The initial neutron excess is $\eta = \frac{1}{6}$ for each expansion; but the differences in final values owing to electron capture are small, so that every expansion has a final η near 0.17, except for $\phi \lesssim 0.002$. The small residual deviations are not enough to influence the 66/48 abundance ratio shown. The short-dashed line is a guide to the eye showing unity.

TABLE 5A

SPECIES AND PROGENITORS FOR $\phi = 0.03$ EXPANSION

^{A}Z	Progenitor	η_{prog}
^{48}Ca	^{48}Ca	0.1667
^{50}Ti	^{50}Ti	0.1200
	^{50}Ca	0.2000
^{54}Cr	^{54}Cr	0.1111
^{66}Zn	^{66}Ni	0.1515
^{70}Zn	^{70}Ni	0.2000
^{79}Br	^{79}Ga	0.2152
	^{79}Cu	0.2658
^{81}Br	^{81}As	0.1852
	^{81}Ga	0.2346
^{82}Se	^{82}Ge	0.2195
	^{82}Zn	0.2863
^{97}Mo	^{97}Br	0.2784

TABLE 5B

SPECIES AND PROGENITORS FOR $\phi = 0.03$ NSE

^{A}Z	Progenitor	η_{prog}
^{48}Ca	^{48}Ca	0.1667
^{50}Ti	^{50}Ti	0.1200
^{54}Cr	^{54}Cr	0.1111
^{66}Zn	^{66}Ni	0.1515
^{70}Zn	^{70}Ni	0.2000
^{78}Se	^{78}Ge	0.1795
	^{78}Zn	0.2308
	^{78}Ni	0.2821
^{80}Se	^{80}Ge	0.2000
	^{80}Zn	0.2500

shown as the dashed curve, have overproduction factors greater than 10^5 but are never the largest overproduction in the range $\eta = 0.1$–0.3 and therefore have been omitted. Figure 17*b* shows the corresponding overproduction factors for NSE with $\phi = 0.03$ at $T_9 = 3.5$. Again in Figure 17*b* only those species that attain the maximum overproduction in the range $\eta = 0.1$–0.3 are shown. The dashed curve in this figure gives the overproduction of ^{48}Ca. Table 5 will help the reader identify the radioactive progenitors of the stable species shown in Figures 17*a* and 17*b*.

Figure 17*b* shows that ^{48}Ca is nowhere the maximum overabundance in NSE for $T_9 = 3.5$ and $\phi = 0.03$. NSE guidelines therefore erroneously lead one to expect large ^{66}Zn/^{48}Ca ratios. On the other hand, Figure 17*a* shows ^{48}Ca is actually the most overabundant isotope in the $\phi = 0.03$ expansions for $\eta \approx 0.14$–0.17. The ^{48}Ca/^{66}Zn overproduction ratio considerably exceeds unity. This is simply a consequence of the freezeout with too many nuclei. The very extended overabundance curve for ^{48}Ca in Figure 17*a* shows that this effect is persistent over a wide range in η; its maximum is broader than the others. Furthermore, at $\eta = 0.24$, the ^{48}Ca shifts over to ^{50}Ca, the progenitor of ^{50}Ti at this η. The system thereby manages to cling to too many nuclei even as the material gets too neutron rich for ^{48}Ca! The reduced ^{66}Zn/^{48}Ca overproduction ratio makes the

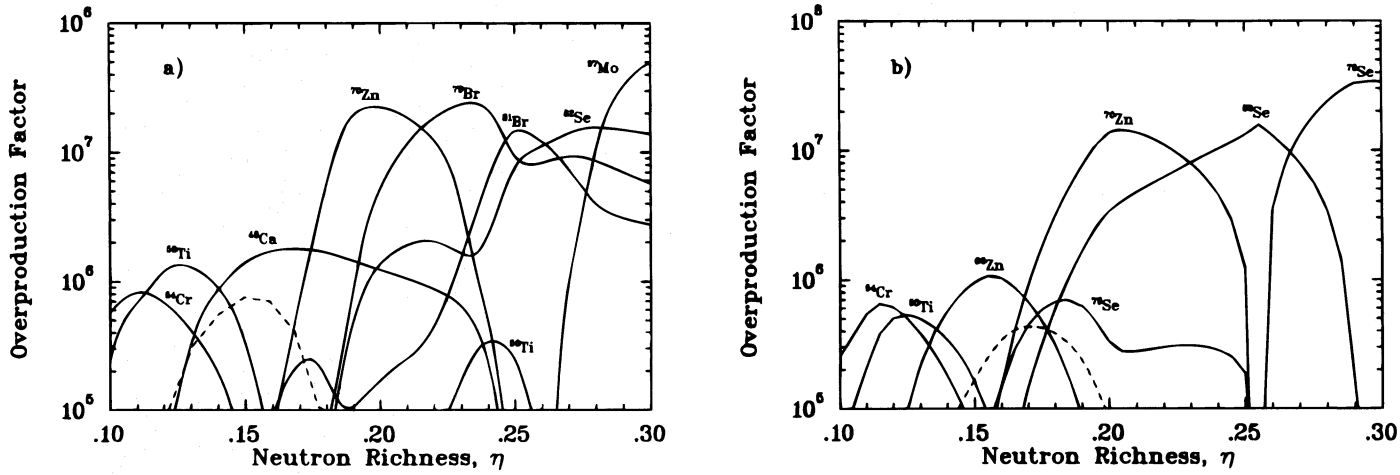

FIG. 17.—Overproduction factors after decay to stable daughter nuclides of selected species as a function of neutron richness for (*a*) $\phi = 0.03$ expansion and (*b*) $\phi = 0.03$ NSE at $T_9 = 3.5$. Only those species that attain the maximum overproduction (compared to all other species) somewhere in the range $\eta = 0.1$–0.3 are shown. Many other species have overproduction factors greater than 10^5 (e.g., ^{66}Zn [*dashed curve*] in [*a*] or ^{48}Ca [*dashed curve*] in [*b*]), but they nowhere have the maximum overproduction and so do not appear in this figure. Weak interactions change η during the expansions. The η chosen for (*a*) is that at $T_9 = 3.5$. The reader may find Table 5 useful in identifying the radioactive progenitors of the species shown in this figure.

observed isotopic excesses in meteorites (Volkening & Papanastassiou 1990; Loss & Lugmair 1990) easier to understand as a nucleosynthetic effect without appealing to loss of ^{66}Zn memory; however, the many inclusions without ^{66}Zn may nonetheless seem to require significant Zn memory loss as well.

The looming specter of the huge ^{70}Zn overproduction will limit any superpositions over η. Although some material with $\eta > 0.17$ is allowed in a superposition, too much will lead to too much ^{70}Zn. The mass excess we have used for ^{70}Ni (-60.136 MeV) is a theoretical extrapolation, since the nuclear data only go out to ^{69}Ni (Tuli 1990). If the real binding of ^{70}Ni were in fact smaller, the overproduction of ^{70}Zn would correspondingly be less. On the other hand, as Woosley & Eastman (1995) point out, it is likely that a kind of β-equilibrium establishes itself during the Type Ia supernovae that probably make ^{48}Ca. This β-equilibrium would naturally keep η from getting much larger than ~ 0.17. Interestingly, the detection (Volkening & Papanastassiou 1990) of excess ^{66}Zn at 16.7 ± 3.7 ϵu in a FUN inclusion EK-1-4-1 was accompanied by a comparable but statistically less secure deficit 21 ± 13 ϵu at ^{70}Zn. A simple admixture to solar matter does not, of course, produce a deficit, so no simple interpretation can be made at this time. But an interesting future for Zn isotopic anomalies can be expected.

For $\eta > 0.2$ in Figure 17*a*, rather rare neutron-rich species appear, while for η approaching 0.3, the matter actually undergoes a mini *r*-process during freezeout to get rid of the last of its free neutrons. These results are probably irrelevant, however, because Type Ia cores are unlikely to get so neutron rich.

Any discussion of neutron-rich isotopic anomalies in CAIs must take into account their macroscopic size, which indicates that CAIs were formed in the solar accretion disk from preexisting components. They are not themselves representative of any stellar source. Their ^{48}Ca, ^{50}Ti, ^{54}Cr, ^{58}Fe, ^{62,64}Ni, and ^{66,70}Zn isotopic anomalies may, via the chemical-memory effects surviving their formation, contain components not only from many Type Ia supernovae but from Type II supernovae as well. Although core-collapse Type II supernovae do not produce significant ^{48}Ca, as we have shown, the intense neutron fluxes in shells of massive stars do greatly enrich ^{50}Ti, ^{54}Cr, ^{58}Fe, and ^{62,64}Ni. This is evident, for example, in the O/Ne shell from the table by Meyer, Weaver, & Woosley (1995). If the CAI chemical memory involves supernova condensates rich in such shell matter, they will decouple ^{48}Ca from those other neutron-rich isotopes. The spectrum of anomalies is more complicated than simply a mean yield from the Type Ia supernovae that synthesize the ^{48}Ca. Nonetheless, it is evident even by inspection that the overabundances from the Type Ia low-entropy expansions generate the leading nuclear component within the spectrum of observed anomalies.

Much work remains in deciphering the clues to the origin of ^{48}Ca, but we have also learned a great deal. ^{48}Ca cannot survive high-entropy expansions because of shifting QSEs with too few nuclei. ^{48}Ca does survive low-entropy expansions because of the freezeout with too many nuclei. ^{48}Ca plays a key role in its own synthesis as the QSE post to which other species tie their abundances. It will be fascinating to see how these hard-won insights into ^{48}Ca synthesis will fit in with future models of astrophysical settings.

This work was supported by NASA grants NAGW-3480 and NAGW-3277 and by the W. M. Keck Foundation. The authors thank H.-T. Janka for helpful comments.

REFERENCES

Anders, E., & Grevesse, N. 1989, Geochim. Cosmochim. Acta, 53, 197
Bao, Z. Y., & Käppeler, F. 1987, At. Data Nucl. Data Tables, 36, 411
Bethe, H. A., & Wilson, J. R. 1985, ApJ, 295, 14
Bodansky, D., Clayton, D. D., & Fowler, W. A. 1968, ApJS, 16, 299
Burbidge, E. M., Burbidge, G. R., Fowler, W. A., & Hoyle, F. 1957, Rev. Mod. Phys., 29, 547
Cameron, A. G. W. 1979, ApJ, 230, L53
Caughlan, G. R., & Fowler, W. A. 1988, At. Data Nucl. Data Tables, 40, 283
Clayton, D. D. 1981, Proc. Lunar Planet. Sci. Conf. 12B, 1781
Cowan, J. J., Thielemann, F.-K., & Truran, J. W. 1991, Phys. Rep., 208, 267
Fuller, G. M., Fowler, W. A., & Newman, M. J. 1980, ApJS, 42, 447
———. 1982a, ApJ, 252, 715
———. 1982b, ApJS, 48, 279
———. 1985, ApJ, 293, 1
Hainebach, K. L., Clayton, D. D., Arnett, W. D., & Woosley, S. E. 1974, ApJ, 193, 157
Hartmann, D., Woosley, S. E., & El Eid, M. F. 1985, ApJ, 297, 837
Lee, T. 1988, in Meteorites and the Early Solar System, ed. J. F. Kerridge & M. S. Matthews (Tucson: Univ. Arizona Press), 1063
Lee, T., Papanastassiou, D. A., & Wasserburg, G. J. 1978, ApJ, 220, L21
Loss, R. D., & Lugmair, G. W. 1990, ApJ, 360, L59
Meyer, B. S. 1993, Phys. Rep., 227, 257
———. 1994, ARA&A, 32, 153
Meyer, B. S., Mathews, G. J., Howard, W. M., Woosley, S. E., & Hoffman, R. 1992, ApJ, 399, 656
Meyer, B. S., Weaver, T. A., & Woosley, S. E. 1995, Meteoritics, 30, 325
Rauscher, T., Applegate, J. A., Cowan, J. J., Thielemann, F.-K., & Wiescher, M. 1994, ApJ, 429, 499
Takahashi, K., Witti, J., & Janka, H.-Th. 1994, A&A, 286, 857
Thielemann, F.-K., Arnould, M., & Truran, J. W. 1987, in Advances in Nuclear Astrophysics, ed. E. Vangioni-Flam, J. Audouze, M. Cassé, J.-P. Chieze, & J. Tran Thahn Van (Gif-sur-Yvette: Editions Frontières), 525
Tuli, J. 1990, Nuclear Wallet Cards (Brookhaven: Brookhaven Natl. Lab.)
Volkening, J., & Papanastassiou, D. A. 1990, ApJ, 258, L29
Weaver, T. A., & Woosley, S. E. 1993, ApJ, 227, 65
Woosley, S. E., Arnett, W. D., & Clayton, D. D. 1973, ApJS, 26, 231
Woosley, S. E., & Eastman, R. G. 1995, preprint
Woosley, S. E., Fowler, W. A., Holmes, J. A., & Zimmerman, B. A. 1975, Tables of Thermonuclear Reaction Rate Data for Intermediate Mass Nuclei (OAP-422), unpublished
Woosley, S. E., & Hoffman, R. D. 1992, ApJ, 395, 202
Woosley, S. E., Wilson, J. R., Mathews, G. J., Hoffman, R. D., & Meyer, B. S. 1994, ApJ, 433, 229